DOI: 10.1002/zaac.201000437

Cadmium(II) Complexes with Mixed *cis*-Epoxysuccinate and 2,2'-Bipyridyl-Like Ligands: Syntheses, Crystal Structures, and Luminescent Properties

Chun-Sen Liu,*[a] Cong Wang,[a] Min Hu,[a] and Shao-Ming Fang*[a]

Keywords: Cadmium; cis-Epoxysuccinate ligand; 2,2'-Bipyridyl-like molecules; Crystal structures; Luminescence

Abstract. Two new Cd^{II} complexes, $[Cd(\mathbf{ces})(phen)]_\infty$ (**1**) and $\{[Cd(\mathbf{ces})(bpy)(H_2O)](H_2O)\}_2$ (**2**), were prepared by slow solvent evaporation methods from mixtures of *cis*-epoxysuccinic acid and $Cd(ClO_4)_2{\cdot}6H_2O$ in the presence of phen or bpy co-ligand (**ces** = *cis*-epoxysuccinate, phen = 1,10-phenanthroline, and bpy = 2,2'-bipyridine). Single-crystal X-ray diffraction analyses show that complex **1** has a one-dimensional (1D) helical chain that is further assembled into a two-dimensional (2D) sheet, and then an overall three-dimensional (3D) network by the interchain C–H···O hydrogen bonds. Complex **2** features a dinuclear structure, which is further interlinked into a 3D supramolecular network by the co-effects of intermolecular C–H···O and C–H···π hydrogen bonds as well as π···π stacking interactions. The structural differences between **1** and **2** are attributable to the intervention of different 2,2'-bipyridyl-like co-ligands. Moreover, **1** and **2** exhibit intense solid-state luminescence at room temperature, which mainly originates from the intraligand π→π* transitions of aromatic co-ligands.

Introduction

Immense interest in metal-organic frameworks (MOFs) originates not only from their intriguing varieties of molecular architectures and topologies but also from their potential applications as functional materials.[1–3] Generally, the structural and functional information of such target materials greatly depends on the selection of the organic tectons and metal atoms, as well as on the reaction pathways. As a consequence, the rational designs of ligands (spacers) and the proper choice of metal ions (nodes) are the main keys to achieve the target coordination polymers.[4–5]

Among various ligands, the versatile carboxylic acid ligands are of especial interest and have been widely used to construct various MOFs.[6–10] In this field, *cis*-epoxysuccinic acid (H_2**ces**) has two chiral centers in the ternary ring backbone as well as a pair of carboxyl groups, which can be regarded as an interesting building tecton in coordination assemblies.[11] On the one hand, it has two carboxyl groups that do not lie in one plane, which provide rich coordination modes and allow it to connect the metal ions in different directions. On the other hand, the oxirane oxygen atom provides additional binding sites, and it can coordinate to the metal ions associated with two near carboxyl oxygen atoms.[6a] In addition, the skilful introduction of 2,2'-bipyridyl-like chelating molecules into the reaction systems involving various carboxylic acid ligands, as auxiliary co-ligands, may generate some interesting coordination architectures. The 2,2'-bipyridyl-like ligands can act as the terminal ligands and provide potential sites for aromatic stacking interactions.[1c,9a,12] In fact, besides coordination bonding, some weak intra- or intermolecular interactions, such as hydrogen-bonding,[13] π···π stacking,[14] and C–H···π[15] interactions also affect the final structures of such complexes, and they may further link discrete subunits or low-dimensional entities into higher-dimensional supramolecular networks.[16]

In our previous work, two magnetic Cu^{II} coordination complexes associated with *cis*-epoxysuccinic acid (H_2**ces**) have been successfully synthesized, which have a 1D helical motif and a neutral isolated Cu_{15} nanocluster under different pH conditions.[11] To further explore the coordination possibilities of H_2**ces** in this contribution, we subsequently chose H_2**ces** as a primary ligand by taking the advantage of the bridging coordination ability of its dicarboxylate groups together with the flexibility of its oxirane ring to construct two Cd^{II} luminescent complexes, by incorporating 1,10-phenanthroline (phen) for $[Cd(\mathbf{ces})(phen)]_\infty$ (**1**) and 2,2'-bipyridine (bpy) for $\{[Cd(\mathbf{ces})(bpy)(H_2O)](H_2O)\}_2$ (**2**), as a chelating co-ligand, respectively. Herein, we report the syntheses, crystal structures, and luminescent properties of these complexes.

Experimental Section

Materials and General Methods: All the starting reagents and solvents for synthesis were commercially available and used as received without further purification. Elemental analyses (C, H, and N) were performed with a Vario EL III Elemental analyzer. The IR spectra were recorded in the range of 4000–400 cm^{-1} with a Tensor 27 OPUS (Bruker) FT-IR spectrometer with KBr pellets. Thermogravimetric

* Dr. C.-S. Liu
E-Mail: chunsenliu@zzuli.edu.cn
* Prof. Dr. S.-M. Fang
E-Mail: smfang@zzuli.edu.cn
[a] Zhengzhou University of Light Industry
Henan Provincial Key Laboratory of Surface & Interface Science
Zhengzhou, Henan 450002, P. R. China
Supporting information for this article is available on the WWW under **http://dx.doi.org/10.1002/zaac.201000437** or from the author.

analysis (TGA) experiments were carried out with a Perkin–Elmer Diamond SII thermal analyzer from room temperature to 900 °C in a nitrogen atmosphere at a heating rate of 10 °C·min^{-1}. The emission/excitation spectra were recorded with an F-7000 (HITACHI) spectrophotometer at room temperature.

Synthesis of Complexes 1 and 2

[Cd(ces)(phen)]$_\infty$ (1): To a methanol solution (2 mL) of H_2**ces** (0.05 mmol) and phen (0.05 mmol), the pH value of which was adjusted by adding dropwise NH_3·H_2O solution (pH = 12.0, at least 0.5 mL), was added a methanol (2 mL) solution of $Cd(ClO_4)_2$·$6H_2O$ (0.05 mmol) with stirring for ca. 5 min. Afterwards, distilled water (2 mL) was added to the resultant colorless suspension with stirring. The mixture was heated in the temperature range of 50–60 °C for ca 5 min and cooled to room temperature. The resulting solution was filtered and a colorless clear filtrate was afforded. Colorless crystals of **1** were obtained by slow evaporation of the solvents after ca. two weeks. Yield ca. 50 % based on H_2**ces**. $C_{16}H_{10}CdN_2O_5$: calcd. C 45.47, H 2.38, N 6.63 %; found: C 45.59, H 2.49, N 6.52 %. **IR** (KBr): $\tilde{\nu}$ = 3447 m(br), 1641 vs, 1584 s, 1518 m, 1495 w, 1428 s, 1391 m, 1341 m, 1295 m, 1221 w, 1138 w, 1100 w, 1070 w, 938 m, 866 m, 847 s, 801 m, 766 m, 728 s, 698 m, 666 w, 643 w cm^{-1}.

{[Cd(ces)(bpy)(H_2O)](H_2O)}$_2$ (2): The same procedure as that for **1** was used with an exception of the introduction of different co-ligand bpy (0.05 mmol) instead of phen in **1**. Colorless crystals of **2** were obtained by slow evaporation of the solvents after ca. one week. Yield ca. 40 % based on H_2**ces**. $C_{14}H_{14}CdN_2O_7$: calcd. C 38.68, H 3.25, N 6.44 %; found: C 38.87, H 3.37, N 6.63 %. **IR** (KBr): $\tilde{\nu}$ = 3447 m(br), 1637 vs, 1508 w, 1475 m, 1440 s, 1351 m, 1294 m, 1249 w, 1158 w, 1061 m, 1020 m, 945 m, 851 w, 806 m, 767 s, 737 m, 684 m, 652 w cm^{-1}.

Caution! Although we have met no problems in handling perchlorate salts during this work, these should be treated cautiously due to their potential explosive nature.

Crystal Structure Determination of 1 and 2

X-ray single-crystal diffraction data for **1** and **2** were collected with an Xcalibur Gemini Eos CCD diffractometer at 293(2) K with Mo-K_α radiation (λ = 0.71073 Å) by ω scan mode. The program SAINT[17] was used for integration of the diffraction profiles. Semi-empirical absorption corrections were applied using SADABS program.[18] All structures were solved by direct methods using the SHELXS program of the SHELXTL package and refined by full-matrix least-squares methods with SHELXL.[19] Metal atoms in each complex were located from the *E*-maps and other non-hydrogen atoms were located in successive difference Fourier syntheses and refined with anisotropic thermal parameters on F^2. Hydrogen atoms of carbon were included in calculated positions and refined with fixed thermal parameters riding on their parent atoms. The hydrogen atoms of water molecules in **2** were located from Fourier difference maps with suitable restraint.

Crystallographic data and experimental details for structural analyses are summarized in Table 1, selected bond lengths and angles as well as hydrogen-bonding arrangements are listed in Table 2, Table 3, and Table 4.

Table 1. Crystal data and structure refinement for **1** and **2**.

	1	**2**
Empirical formula	$C_{16}H_{10}CdN_2O_5$	$C_{14}H_{14}CdN_2O_7$
Formula weight	422.67	434.68
Crystal system	Orthorhombic	Triclinic
Space group	$Pna2_1$	$P\bar{1}$
a /Å	7.8052(3)	7.8751(5)
b /Å	20.0556(8)	10.2477(6)
c /Å	9.3307(3)	10.4366(2)
α /°	90	75.493(5)
β /°	90	80.300(5)
γ /°	90	76.275(5)
V /Å^3	1460.61(9)	786.77(9)
Z	4	2
D /Kg·m^{-3}	1.922	1.835
μ /mm^{-1}	1.526	1.428
R_{int}	0.0232	0.0280
GOF	1.007	0.956
T /K	293(2)	293(2)
R_1[a]/wR_2[b] [$I > 2\sigma(I)$]	0.0221/0.0254	0.0271/0.0306
ρ_{max}/ρ_{min} /e·Å^{-3}	0.449 / –0.260	0.551 / –0.483

a) $R_1 = \Sigma(||F_o|-|F_c||)/\Sigma|F_o|$. b) $wR_2 = [\Sigma w(|F_o|^2-|F_c|^2)^2/\Sigma w(F_o^2)^2]^{1/2}$, where F_o = observed and F_c = calculated structure factors, respectively.

CCDC-804496 and CCDC-804497 contain the supplementary crystallographic data for **1** and **2**, respectively. These data can be obtained free of charge via http://www.ccdc.cam.ac.uk/conts/retrieving.html, or from the Cambridge Crystallographic Data Centre, CCDC, 12 Union Road, Cambridge CB2 1EZ, UK (Fax: +44-1223-336-033; or E-mail: deposit@ccdc.cam.ac.uk)

X-ray Powder Diffraction Studies of 1 and 2

The X-ray powder diffraction (XRPD) patterns of **1** and **2** were recorded at 293 K with a Bruker D8 Advance diffractometer (Cu-K_α, λ = 1.54056 Å) operated at 40 kV and 30 mA, using a copper-target tube and a graphite monochromator. The crushed single-crystalline powder samples were prepared by crushing the crystals and the intensity data were recorded by continuous scan in a $2\theta/\theta$ mode from 3° to 80° with a step size of 0.02° and a scan speed of 2°·min^{-1}. Simulation of the XRPD patterns was carried out by the single-crystal data and diffraction-crystal module of the Mercury (Hg) program available free of charge via the internet at http://www.iucr.org.

Supporting Information (see footnote on the first page of this article): Scheme of coordination modes of the fully deprotonated **ces** ligand in complexes **1** and **2**. XRPD patterns and Thermogravimetric analysis (TGA) plots for **1**–**2**. Solid excitation/emission spectra of the auxiliary phen and bpy ligands at room temperature.

Results and Discussion

Synthesis and General Characterizations

For the investigation of the coordination features of H_2**ces**, our strategy is to prepare two Cd^{II} complexes by changing the 2,2'-bipyridyl-like chelating co-ligands (phen and bpy herein). Two new Cd^{II} complexes were obtained by direct combination of the Cd^{II} salt and H_2**ces** together with different auxiliary co-ligands, followed by solvent evaporation under ambient condi-

Table 2. Selected bond lengths /Å and angles /° for **1**.

Cd1–O4	2.191(3)	Cd1–N2	2.328(4)
Cd1–O2$^{\#1}$	2.251(3)	Cd1–O1	2.346(3)
Cd1–N1	2.296(3)	Cd1–O5	2.504(3)
Cd1$^{\#2}$–O2	2.251(3)		
O4–Cd1–O2$^{\#1}$	100.26(11)	N1–Cd1–O1	152.31(12)
O4–Cd1–N1	110.70(12)	N2–Cd1–O1	86.09(12)
O2$^{\#1}$–Cd1–N1	102.74(11)	O4–Cd1–O5	72.78(11)
O4–Cd1–N2	155.16(12)	O2$^{\#1}$–Cd1–O5	167.27(9)
O2$^{\#1}$–Cd1–N2	103.21(12)	N1–Cd1–O5	89.80(11)
N1–Cd1–N2	71.86(14)	N2–Cd1–O5	82.63(11)
O4–Cd1–O1	82.53(11)	O1–Cd1–O5	70.47(10)
O2$^{\#1}$–Cd1–O1	98.39(10)		

Symmetry transformations used to generate equivalent atoms: #1 = –*x*+4, –*y*+3, *z*+1/2; #2 = –*x*+4, –*y*+3, *z*–1/2.

Table 3. Selected bond lengths /Å and angles /° for **2**.

Cd1–O1	2.2652(18)	Cd1–O3	2.4008(19)
Cd1–N2	2.327(2)	Cd1–O6	2.4074(19)
Cd1–O3$^{\#1}$	2.3276(19)	Cd1–O5	2.6345(18)
Cd1–N1	2.329(2)		
O1–Cd1–N2	96.46(8)	N2–Cd1–O6	80.70(7)
O1–Cd1–O3$^{\#1}$	107.43(6)	O3$^{\#1}$–Cd1–O6	82.02(7)
N2–Cd1–O3$^{\#1}$	148.42(7)	N1–Cd1–O6	115.18(7)
O1–Cd1–N1	154.22(7)	O3–Cd1–O6	140.79(6)
N2–Cd1–N1	70.41(8)	O1–Cd1–O5	69.36(6)
O3$^{\#1}$–Cd1–N1	93.71(7)	N2–Cd1–O5	72.73(7)
O1–Cd1–O3	81.78(7)	O3$^{\#1}$–Cd1–O5	134.80(6)
N2–Cd1–O3	136.82(8)	N1–Cd1–O5	85.34(6)
O3$^{\#1}$–Cd1–O3	68.61(8)	O3–Cd1–O5	66.31(6)
N1–Cd1–O3	92.79(7)	O6–Cd1–O5	138.52(6)
O1–Cd1–O6	82.99(6)		

Symmetry transformations used to generate equivalent atoms: #1 = –*x*, –*y*, –*z*+1.

Table 4. Hydrogen-bonding arrangement /Å and ° for **1** and **2**.

D–H···A	*d*(D–H)	*d*(H···A)	*d*(D···A)	D–H···A
1				
C3–H3A···O2^{a}	0.98	2.56	3.379(5)	141
C7–H7A···O3^{b}	0.93	2.58	3.341(7)	139
C10–H10A···O5^{c}	0.93	2.52	3.221(5)	133
2				
C8–H8A···O4^{a}	0.93	2.55	3.458(8)	166
C12–H12A···O2^{a}	0.93	2.57	3.346(5)	140
O6–H1W···O7^{b}	0.85	1.82	2.656(6)	169
O7–H3W···O2^{c}	0.85	1.82	2.657(6)	169
C4–H4A···*Cg*1^{d}	0.98	2.77	3.534(1)	135

Symmetry codes for **1**: a = –*x*+5, –*y*+3, *z*+1/2; b = –*x*+9/2, *y*+1/2, *z*+1/2; c = *x*–1/2, –*y*+7/2, *z*. Symmetry codes for **2**: a = *x*, *y*+1, *z*; b = *x*–1, *y*, *z*; c = –*x*+1, –*y*, –*z*; d = –*x*+1, –*y*, –*z*+1. *Cg*1 is the centroid of the N1/C5–C9 pyridyl ring of bpy ligand.

tions. It should be pointed out that the use of excess $NH_3{\cdot}H_2O$ solution is a key point for the formation of **1** and **2**, which adjusts the pH values of the reaction systems. As such, we have not obtained any complexes suitable for X-ray analysis when using other basic organic/inorganic compounds instead of $NH_3{\cdot}H_2O$, such as Et_3N, pyridine, 2,6-dimethylpyridine, and NaOH.

Complexes **1** and **2** are air stable and all general characterizations were carried out by using the crushed single-crystal samples. The IR spectra usually show features attributable to each component of the complexes. In the IR spectrum of **2**, the broad band centered at 3447 cm^{-1} indicates O–H stretching of coordinated/lattice water molecules. As a matter of fact, the IR absorption of the carboxylate group is very complicated due to its coordination diversity with metal ions. The characteristic bands of carboxylate groups in **1** and **2** appeared in the usual region at 1641–1584 cm^{-1} for the antisymmetric stretching vibrations and at 1440–1428 cm^{-1} for the symmetric stretching vibrations. Furthermore, the Δv values [$\Delta v = v_{asym}(COO^-) - v_{sym}(COO^-)$] of 156 and 213 cm^{-1} for **1** and 162 and 197 cm^{-1} for **2**, respectively, are in good agreement with their solid structural features from the results of their crystal structures.[20]

Zeitschrift für anorganische und allgemeine Chemie ZAAC Journal of Inorganic and General Chemistry

Descriptions of Crystal Structures of 1 and 2

[Cd(ces)(phen)]$_\infty$ (1)

2,2'-Bipyridyl-like molecules are classic bidentate chelating ligands, such as phen and bpy, which can commonly act as terminal ligands, and also may provide supramolecular interaction sites for molecular recognition or assembly.[1c,9a,12] Accordingly, the reaction of $Cd(ClO_4)_2 \cdot 6H_2O$ with H_2**ces** ligand in the presence of phen, as a chelating co-ligand, lead to the formation of **1**, which consists of 1D helical chains. As illustrated in Figure 1a, each asymmetric unit in **1** contains one crystallographically unique Cd^{II} atom, one fully deprotonated **ces** ligand, and one chelating phen ligand. In the helical chain, each distorted octahedral Cd^{II} atom is defined by four oxygen atoms [Cd–O1/2/4/5: 2.191(3)–2.504(3) Å] from two distinct **ces** ligands (three oxygen atoms from the carboxylate groups and one oxygen atom from the oxirane ring, here O5, see Figure 1a) and two N-donor atoms [Cd–N1/2: 2.296(3)–2.328(4) Å] from one phen molecule. In **1**, each **ces** ligand uses its four oxygen atoms [three oxygen atoms from two carboxylate groups and one oxygen atom from the oxirane ring, see Figure 1a] to coordinate to two Cd^{II} atoms and adopt two different coordination modes: namely μ_2-η^1:η^1-*syn-anti*-bridging and μ_1-η^1:η^0-monodentate modes (see Scheme S1a in the Supporting Information). In other words, each **ces** ligand uses its two carboxylate groups in a *cis* conformation on the oxirane ring to connect two Cd^{II} atoms, forming a left-handed and a right-handed helical array along the [001] axis with a period of 9.331(6) Å.

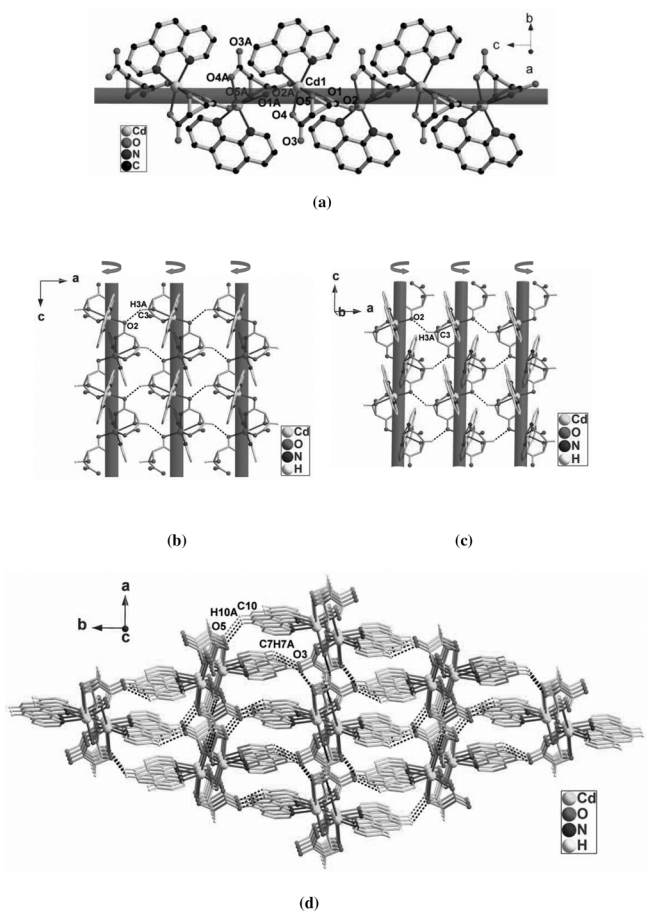

Figure 1. View of (a) the 1D helical coordination chain along the [001] direction, showing the local coordination environment of Cd^{II} in **1** (symmetry code: A = 4–*x*, 3–*y*, 0.5+*z*), (b) and (c) two distinct 2D sheets running parallel to *ac* planes, respectively, formed by the interchain C–H···O hydrogen bonds, and (d) the 3D network along the *c* axis, formed by the interlayer C–H···O hydrogen-bonds.

Furthermore, adjacent 1D helical chains are linked together to afford two different 2D sheets, running along the *ac* planes (see Figure 1b,c) by the interchain C–H···O hydrogen bonds[21] (C3–H3A···O2^a, symmetry code a = –*x*+5, –*y*+3, *z*+0.5, see Table 4 for detailed information). In addition, adjacent 2D layers are assembled into a 3D supramolecular framework by the interlayer C–H···O hydrogen-bonds between **ces** and phen ligands [C7–H7A···O3^b and C10–H10A···O5^c; symmetry codes b = –*x*+4.5, *y*+0.5, *z*+0.5 and c = *x*–0.5, –*y*+3.5, *z*; see Figure 1d and Table 4 for detailed information].

{[Cd(ces)(bpy)(H$_2$O)](H$_2$O)}$_2$ (2)

Compared to phen, bpy has a smaller conjugated π system resulting from the steric size of its aromatic skeleton and is more likely to chelate metal ions, which in turn terminates the coordination sites around the metal atoms.[1c,9a] When bpy was introduced into the assembled system instead of phen, different from **1**, the centrosymmetric dinuclear complex **2** was produced (see Figure 2). In the asymmetric unit, each Cd^{II} atom is located in a seven-coordinate distorted pentagonal bipyramidal environment, being surrounded by a pair of $N_{pyridyl}$ atoms of bpy ligand, four oxygen atoms from two **ces** ligands (three oxygen atoms from the carboxylate groups and one oxygen atom from the oxirane ring, see Figure 2a), and one oxygen atom of the water ligand (see Table 3 for detailed bond parameters). As shown in Figure 2a, one carboxylate group of each **ces** ligand acts in a μ_1-η^1:η^0-monodentate mode whereas the other adopts a μ_2-η^2:η^0-bridging mode (see Scheme S1b in the Supporting Information). Furthermore, adjacent Cd^{II} atoms are connected by two μ_2-η^2:η^0-bridging carboxylate groups from two different **ces** ligands to give rise to the formation of the final dinuclear structure.

In addition, adjacent dinuclear [Cd(**ces**)(bpy)(H$_2$O)]$_2$ units are extended into a 1D chain along the [010] direction by the co-effects of intermolecular C–H···O hydrogen bonds (C8–H8A···O4^a and C12–H12A···O2^a; symmetry code a = *x*, 1 + *y*, *z*) and π···π stacking interactions between the completely parallel pyridyl rings of adjacent bpy ligands, with a centroid–centroid separation of 3.761 Å (see Figure 2b).[22] Moreover, these 1D motifs are further interlinked by the intermolecular C–H···π supramolecular interactions between **ces** and bpy ligands with an edge-to-face orientation[15,23] (d = 2.77 Å; A = 135°) to generate a 2D layer running parallel to the *ab* plane. Finally, further investigation of crystal packing reveals that these parallel 2D layers are interlinked to lead to the formation of an overall 3D network by the interlayer C–H···O hydrogen bonds (O6–H1W···O7^b and O7–H3W···O2^c, symmetry codes

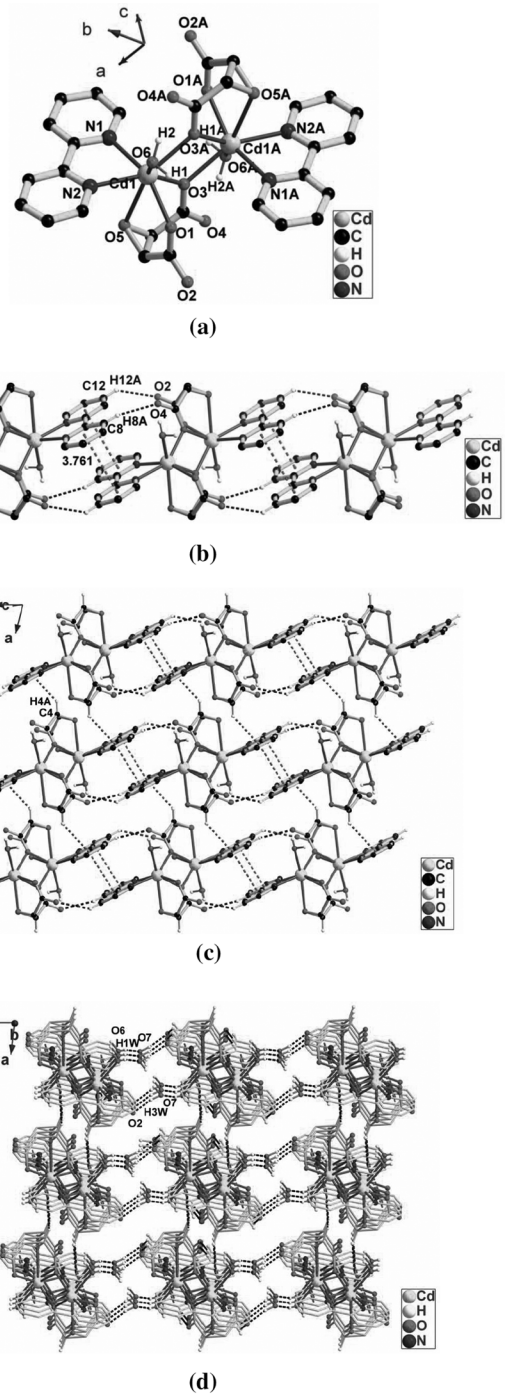

Figure 2. View of (a) the local coordination environment of Cd^{II} (symmetry code: A = –*x*, –*y*, 1–*z*), (b) the 1D chain in **2**, running along the [010] direction, formed by the C–H···O hydrogen bonds and intermolecule π···π stacking interactions, (c) the 2D network, running parallel to *ab* plane, formed by the interchain C–H···π supermolecular interactions, and (d) the 3D network, viewed along the *b* axis, formed by the intermolecular C–H···O hydrogen-bonds.

b = –1+*x*, *y*, *z* and *c* = 1–*x*, –*y*, –*z*; see Table 4 for detailed information) along [001] (see Figure 2d).

XRPD Results

To confirm whether the crystal structures are truly representative of the bulk materials for the further luminescence measurements, X-ray powder diffraction (XRPD) experiments have been carried out for the phase purities of samples **1** and **2**. The XRPD experimental and computer-simulated patterns of the corresponding complexes are shown in Figure S1 (Supporting Information). Although the experimental patterns have a few unindexed diffraction lines and some are slightly broadened in comparison with those simulated from the single crystal modes, it still can be considered favorably that the bulk synthesized materials and the as-grown crystals are homogeneous for **1** and **2**.

Thermogravimetric Analysis

Thermal gravimetric analysis (TGA) experiments of **1** and **2** were performed in a nitrogen atmosphere by heating the corresponding complex from room temperature to 900 °C with a heating rate of 10 °C·min^{-1} (Figure S2 in the Supporting Information). Complex **1** is stable up to ca. 280 °C. With that, the decomposition of the components occurs with two consecutive steps of weight loss on approaching 300 °C (maxima at 308 and 554 °C). The weight loss of 71.90 % observed from 280 to 600 °C is very close to the calculated value of 73.41 %, which corresponds to the components of phen and **ces** ligands. The final residue is not characterized because its weight loss does not stop until heating ends at 900 °C. In the case of **2**, the first weight loss of 7.96 % (calcd. 8.12 %) in the range of 40–110 °C corresponds to the removal of the lattice and coordinated water molecules. The remaining substance is stable up to ca. 210 °C. With that, the decomposition of the residuary components occurs with three consecutive steps of weight loss (maxima at 276, 326, and 492 °C) in the TGA curve, which also recorded the weight loss processes of the relevant, various components in **2**.

Luminescent Properties

The emission spectra of **1** and **2** in the solid state at room temperature are shown in Figure 3. Excitation of the microcrystalline samples of **1** and **2** at 348 and 337 nm produces the intense luminescence with peak maxima at 373 and 347 nm, respectively. To further analyze the nature of these emission bands, the luminescent properties of H_2**ces** and auxiliary co-ligands (phen and bpy) were also investigated under the same experimental conditions. H_2**ces** ligand has almost no contribution to the luminescent emission in **1** and **2** in the range of 300–400 nm. In contrast, the auxiliary phen and bpy ligand shows the luminescent emissions obviously in the solid state (Figure S3 in the Supporting Information).[16a,9c] By comparing the locations and profiles of their excitation/emission peaks with those of **1** and **2**, we can presume that these emissions are neither metal-to-ligand charge transfer (MLCT) nor ligand-to-metal charge transfer (LMCT) in nature, because the Cd^{II} ion with d^{10} configuration is difficult to oxidize or to reduce[12b,16a] and should mainly be ascribed to the intraligand π→π* transitions, namely, ligand-to-ligand charge transfer (LLCT) of auxiliary co-ligand.[24] Also, the different emissions

Zeitschrift für anorganische und allgemeine Chemie ZAAC Journal of Inorganic and General Chemistry

in **1** and **2** may result from the intervention of different 2,2'-bipyridyl-like chelating co-ligands.

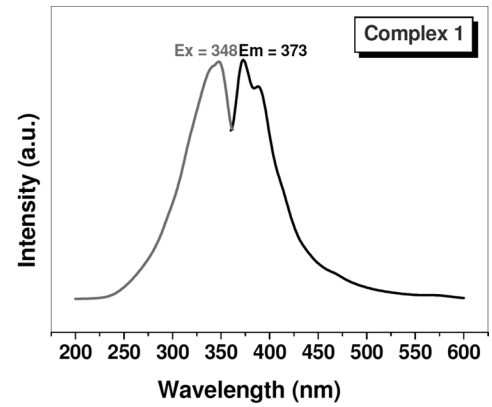

(a)

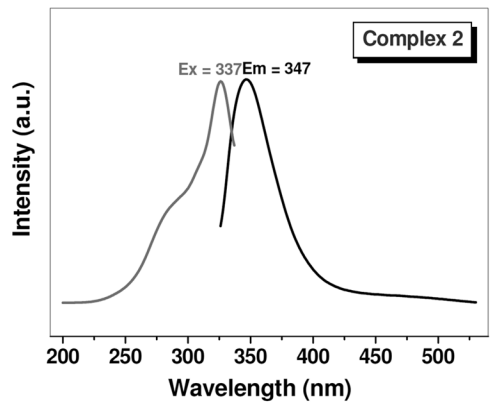

(b)

Figure 3. Solid-state excitation/emission spectra of **1** (a) and **2** (b) at room temperature.

Conclusions

Two new Cd^{II} complexes with 1D helical and dinuclear structures were obtained by the reaction of *cis*-epoxysuccinic acid and Cd^{II} salt, together with incorporating different chelating co-ligands, phen for **1** and bpy for **2**. The presented results demonstrate that the different 2,2'-bipyridyl-like co-ligand (phen or bpy) may play an important role in governing final structures. Complexes **1** and **2** show luminescent emission at room temperature, mainly due to the intraligand $\pi \rightarrow \pi^*$ transitions of aromatic auxiliary co-ligands. Finally, the present findings will further prompt us to construct more functional crystalline solids with intriguing structures and potentially useful properties through such a reliable procedure described here by employing the analogous alicyclic or heteroalicyclic multicarboxylic acids.

Acknowledgement

This work was supported by the *National Natural Science Foundation of China* (Grant Nos. 20801049 and 21071129) and *Henan Outstanding Youth Science Fund* (to *C.S.L.*).

References

[1] a) H. Liang, Y. He, Y. Ye, X. Xu, F. Cheng, W. Sun, X. Shao, Y. Wang, J. Li, K. Wu, *Coord. Chem. Rev.* **2009**, *253*, 2959; b) W. L. Leong, J. J. Vittal, *Chem. Rev.* **2011**, *111*, 688; c) B.-H. Ye, M.-L. Tong, X.-M. Chen, *Coord. Chem. Rev.* **2005**, *249*, 545; d) G. E. Kostakis, A. K. Powell, *Coord. Chem. Rev.* **2009**, *253*, 2686; e) J. J. Perry IV, J. A. Perman, M. J. Zaworotko, *Chem. Soc. Rev.* **2009**, *38*, 1400.

[2] a) M. Du, X.-J. Jiang, X.-J. Zhao, *Inorg. Chem.* **2007**, *46*, 3984; b) X. Xu, X. Zhang, X. Liu, T. Sun, E. Wang, *Cryst. Growth Des.* **2010**, *10*, 2272.

[3] a) R. Robson, *Dalton Trans.* **2008**, 5113; b) J. Zhao, L. Mi, J. Hu, H. Hou, Y. Fan, *J. Am. Chem. Soc.* **2008**, *130*, 15222; c) Z.-X. Li, T.-L. Hu, H. Ma, Y.-F. Zeng, C.-J. Li, M.-L. Tong, X.-H. Bu, *Cryst. Growth Des.* **2010**, *10*, 1138; d) C. Yue, C. Yan, R. Feng, M. Wu, L. Chen, F. Jiang, M. Hong, *Inorg. Chem.* **2009**, *48*, 2873.

[4] a) M. Du, Z.-H. Zhang, L.-F. Tang, X.-G. Wang, X.-J. Zhao, S. R. Batten, *Chem. Eur. J.* **2007**, *13*, 2578; b) S. Kitagawa, R. Kitaura, S. Noro, *Angew. Chem. Int. Ed.* **2004**, *43*, 2334; c) C.-S. Liu, J.-J. Wang, Z. Chang, L.-F. Yan, X.-H. Bu, *CrystEngComm* **2010**, *12*, 1833.

[5] a) R. Banerjee, A. Phan, B. Wang, C. Knobler, H. Furukawa, M. O'Keeffe, O. M. Yaghi, *Science* **2008**, *319*, 939; b) L. Ma, C. Abney, W. Lin, *Chem. Soc. Rev.* **2009**, *38*, 1248.

[6] a) D. Sun, N. Zhang, R.-B. Huang, L.-S. Zheng, *Cryst. Growth Des.* **2010**, *10*, 3699; b) C.-M. Jin, L.-Y. Wu, H. Lu, Y. Xu, *Cryst. Growth Des.* **2008**, *8*, 215; c) Z.-J. Lin, M.-L. Tong, *Coord. Chem. Rev.* **2011**, *255*, 421.

[7] a) Y.-Q. Lan, S.-L. Li, J.-S. Qin, D.-Y. Du, X.-L. Wang, Z.-M. Su, Q. Fu, *Inorg. Chem.* **2008**, *47*, 10600; b) Z.-M. Zhang, S. Yao, Y.-G. Li, R. Clérac, Y. Lu, Z.-M. Su, E.-B. Wang, *J. Am. Chem. Soc.* **2009**, *131*, 14600; c) H.-Y. Bai, J.-F. Ma, J. Yang, Y.-Y. Liu, H.-Wu, J.-C. Ma, *Cryst. Growth Des.* **2010**, *10*, 995.

[8] a) M. Eddaoudi, J. Kim, N. Rosi, D. Vodak, J. Wachter, M. O'Keeffe, O. M. Yaghi, *Science* **2002**, *295*, 469; b) J. L. C. Rowsell, A. R. Millward, K. S. Park, O. M. Yaghi, *J. Am. Chem. Soc.* **2004**, *126*, 5666.

[9] a) C.-S. Liu, X.-S. Shi, J.-R. Li, J.-J. Wang, X.-H. Bu, *Cryst. Growth Des.* **2006**, *6*, 656; b) W.-T. Liu, Y.-C. Ou, Y.-L. Xie, Z. Lin, M.-L. Tong, *Eur. J. Inorg. Chem.* **2009**, 4213; c) C.-S. Liu, E. C. Sañudo, M. Hu, L.-M. Zhou, L.-Q. Guo, S.-T. Ma, L.-J. Gao, S.-M. Fang, *CrystEngComm* **2010**, *12*, 853.

[10] D.-R. Xiao, Y.-G. Li, E.-B. Wang, L.-L. Fan, H.-Y. An, Z.-M. Su, L. Xu, *Inorg. Chem.* **2007**, *46*, 4158.

[11] S.-M. Fang, Q. Zhang, M. Hu, E. C. Sañudo, M. Du, C.-S. Liu, *Inorg. Chem.* **2010**, *49*, 9617.

[12] a) J.-M. Lehn, *Supramolecular Chemistry*; VCH, Weinheim, Germany **1995**; b) L.-F. Ma, C.-P. Li, L.-Y. Wang, M. Du, *Cryst. Growth Des.* **2010**, *10*, 2641.

[13] a) G. R. Desiraju, T. Steiner, *The Hydrogen Bond in Structural Chemistry and Biology*, Oxford University Press, Oxford, **1999**; b) G. Barberà, C. Viñas, F. Teixidor, G. M. Rosair, A. J. Welch, *J. Chem. Soc., Dalton Trans.* **2002**, 3647.

[14] a) C. Janiak, *J. Chem. Soc., Dalton Trans.* **2000**, 3885; b) A. L. Spek, PLATON, *A Multipurpose Crystallographic Tool*, Utrecht University: Utrecht, The Netherlands, **2005**.

[15] M. Nishio, Y. Umezawa, K. Honda, S. Tsuboyama, H. Suezawa, *CrystEngComm* **2009**, *11*, 1757.

[16] a) S.-M. Fang, Q. Zhang, M. Hu, X.-G. Yang, L.-M. Zhou, M. Du, C.-S. Liu, *Cryst. Growth Des.* **2010**, *10*, 4773; b) C.-S. Liu, M. Hu, S.-T. Ma, Q. Zhang, L.-M. Zhou, L.-J. Gao, S.-M. Fang, *Aust. J. Chem.* **2010**, *63*, 463.

[17] *SAINT Software Reference Manual*; Bruker AXS: Madison, WI, **1998**.

[18] G. M. Sheldrick, *SADABS*, Siemens Area Detector Absorption Corrected Software, University of Göttingen, Göttingen, Germany, **1996**.

[19] a) G. M. Sheldrick, *SHELXTL NT Version 5.1*, Program for Solution and Refinement of Crystal Structures, University of Göttin-

gen, Göttingen, Germany, **1997**; b) G. M. Sheldrick, *Acta Crystallogr., Sect. A* **2008**, *64*, 112.
[20] K. Nakamoto, *Infrared and Raman Spectra of Inorganic and Donor Hydrogen Bond Coordination Compounds*, John Wiley & Sons, New York, **1986**.
[21] a) M. J. Calhorda, *Chem. Commun.* **2000**, 801; b) P. Hobza, Z. Havlas, *Chem. Rev.* **2000**, *77*, 4253.
[22] C. A. Hunter, J. K. M. Sanders, *J. Am. Chem. Soc.* **1990**, *112*, 5525.
[23] a) M. Nishio, Y. Umezawa, K. Honda, S. Tsuboyama, H. Suezawa, *CrystEngComm* **2009**, *11*, 1757; b) M. Nishio, M. Hirota, Y. Umezawa, *A Comprehensive Monograph: The C–H···π Interaction Evidence, Nature and Consequences*, Wiley-VCH, NewYork, **1998**.
[24] a) L.-L. Wen, D.-B. Dang, C.-Y. Duan, Y.-Z. Li, Z.-F. Tian, Q.-J. Meng, *Inorg. Chem.* **2005**, *44*, 7161; b) S. Wang, Y. Hou, E. Wang, Y. Li, L. Xu, J. Peng, S. Liu, C. Hu, *New J. Chem.* **2003**, *27*, 1144; c) X. Meng, Y. Song, H. Hou, H. Han, B. Xiao, Y. Fan, Y. Zhu, *Inorg. Chem.* **2004**, *43*, 3528.

Received: December 14, 2010
Published Online: March 22, 2011

